Eur. Phys. J. E **3**, 45–53 (2000)

THE EUROPEAN PHYSICAL JOURNAL E

EDP Sciences

Ordering of urchin-like charged copolymer micelles: Electrostatic, packing and polyelectrolyte correlations

F. Muller[1,a], M. Delsanti[2], L. Auvray[3], J. Yang[4], Y.J. Chen[4,b], J.W. Mays[4], B. Demé[5], M. Tirrell[6,c], and P. Guenoun[1,d]

[1] Service de Physique de l'Etat Condensé, CEA Saclay, F-91191 Gif-sur-Yvette Cedex, France
[2] Service de Chimie Moléculaire, CEA Saclay, F-91191 Gif-sur-Yvette Cedex, France
[3] Laboratoire Léon Brillouin, CEA Saclay, F-91191 Gif-sur-Yvette Cedex, France
[4] Department of Chemistry, University of Alabama at Birmingham, Birmingham, AL 35294, USA
[5] Institut Laue-Langevin, BP 156, F-38042 Grenoble Cedex, France
[6] Department of Chemical Engineering and Materials Science, University of Minnesota, Minneapolis, MN 55455, USA

Received 8 October 1999

Abstract. We report the results of small-angle neutron scattering (SANS) studies on aqueous solutions of spherical polyelectrolyte micelles formed by association of charged-neutral diblock copolymers. The neutral moieties are found to self-assemble into small dense spheres (cores of the micelles) whose sizes are independent of the polymer concentration c. In the dilute regime, $c < c^*$, where c^* is the overlap concentration of the micelles, the conformation of the charged groups, which form the corona of the micelles, is found to be extended. A liquid-like order is observed over a wide concentration range spanning from the dilute regime to the concentrated regime. For $c > c^*$, polyelectrolyte correlations appear at smaller spatial scales and coexist with the liquid-like order. These results suggest that for dense brushes, above c^*, the rod-like statistics of the charged chains begin to disappear due to contraction of corona arms or by interpenetration of coronae. For less dense brushes, the charged chains are found to be extended up to concentrations far above c^*, before the progressive development of polyelectrolyte correlations.

PACS. 61.25.Hq Macromolecular and polymer solutions; polymer melts; swelling – 83.70.Hq Heterogeneous liquids: suspensions, dispersions, emulsions, pastes, slurries, foams, block copolymers, etc. – 82.70.Dd Colloids

1 Introduction

Neutral diblock copolymers have been extensively studied for a long time but only a few experiments are now available on charged-neutral diblock copolymers [1–5]. The interest in the study of such polymers is their water solubility and the extended conformation of the charged moiety, since a fully charged chain is predicted to adopt a rod-like conformation [6] because of the electrostatic repulsion between monomers. In a selective solvent such as water or on a selective surface, these copolymers can self-assemble into a large range of morphologies.

In water, asymmetric fully charged-neutral diblock copolymers made of a long and fully charged moiety (polyelectrolyte) and of a short neutral moiety are expected to form spherical micelles [7]. These spherical micelles are composed of a small dense core formed by the association and collapse of the neutral segments. The charged segments are tethered to this core forming a large spherical corona.

Micellar solutions of charged-neutral copolymers represent a good model of colloids protected by tethered polyelectrolyte chains, grafted or end-adsorbed at the surface of the particles [8,9]. Such stabilization is believed to be very insensitive to the addition of salt, an important requirement for applications. Indeed, we recently showed that the corona of the micelles undergo a weak change of conformation when a rather high salinity level is exceeded [10]. Moreover, for liquid-like structured solutions (see below), the correlations are also weakly sensitive to the addition of salt [4]. On the contrary, colloids stabilized only by their own surface charge are known to be very sensitive to the ionic strength of the solvent. These diblocks are also of wide industrial and ecological relevance, due to the increased need for water solvated systems.

These micellar solutions also are of great fundamental interest. Indeed, many unresolved problems remain

[a] e-mail: muller@spec.saclay.cea.fr
[b] *Present address*: Exxon Chemical Co. Baytown, TX 77522, USA.
[c] *Present address*: Departments of Chemical Engineering and of Materials, University of California, Santa Barbara, CA 93106 USA.
[d] e-mail: guenoun@spec.saclay.cea.fr

concerning charged chains [11,12]. The understanding of polyelectrolyte brushes, where the typical distance between neighboring chains is less than the chain size in solution, may help in clarifying such problems. In aqueous solutions of asymmetric charged-neutral diblock copolymers, the corona can be viewed as a polyelectrolyte brush in a spherical geometry [8,13]. The contraction of this corona upon addition of salt may give insight on the behavior of the persistence length L_p of polyelectrolytes as a function of salt. Since chains in the corona were shown to stay quite rigid in the high salt limit [10], such a concept of persistence length seems relevant and the very weak contraction of the corona should be quantitatively understandable as a dependence of L_p on the added salt concentration S.

Another highly debated subject about polyelectrolytes is the concept of counterion condensation [14–19] which has been mainly examined for isolated chains, but whose application to concentrated chains may lead to effective attractions between chains of like charge [16–19]. Polyelectrolyte brushes, due to their high chain density, may be ideal systems to test such behavior, in particular by inspection of the counterion distribution within the brush [20].

The aim of this paper is to report a study of such micellar solutions by neutron scattering in the dilute and concentrated regimes in order to better characterize their behavior. We checked the association of copolymers using the contrast variation method in solvents which make only the neutral group visible. The scattered signal is found to be consistent with the scattering of spheres with a concentration-independent size. The aggregation number of the micelles is then evaluated by a simple model of the core as a dense polymer melt. The overlap concentration of the micelles is deduced by coupling the aggregation number with dynamic light scattering (DLS) measurements of the hydrodynamic radius of the whole micelle. The structure of the charged group is investigated in the dilute regime in solvents which make only the charged moiety visible. The conformation of charged chains, which form the corona, is found to be nearly fully extended. We observe, at large scale, that such objects are strongly ordered by electrostatic interactions even in the dilute regime. We show the existence of liquid-like order, due to electrostatic and/or packing correlations, over a wide concentration range spanning from the dilute regime to the concentrated regime. At high concentration, polyelectrolyte correlations appear and coexist with the liquid-like order. We discuss the origin of the latter correlations in terms of inter-coronae origin or intra-corona origin. Finally, we examine the structure of the solutions as a function of the brush density.

2 Experimental section

2.1 Materials

We used asymmetric diblock copolymers made of fully deuterated sodium poly(styrene sulfonate) ($NaPSS_d$) and of poly(ethylene-alt-propylene) (PEP) or of poly(tert-butyl-styrene) (PtBS). These materials were synthesized by anionic polymerization [21] according to a method described in reference [7]. Degrees of polymerization for a $NaPSS_d$-PEP copolymer and a $NaPSS_d$-PtBS copolymer of 251-52 and 590-43 were obtained, respectively. In this article, these copolymers will be designed by 251/52 and 590/43. Polydispersities as low as $M_W/M_N = 1.04$ and 1.03 were found, respectively, and high sulfonation rates of 90% and of 80% were measured, respectively, by elemental analysis. Solutions were prepared in dual solvents of deionized H_2O water (MilliQ Millipore system, $18\,M\Omega cm^{-1}$) and pure D_2O. Mixtures were designed to yield solvents whose scattering length density are identical to that of the PEP group (mixture with 4% by volume in D_2O), to that of the PtBS group (mixture with 16% by volume in D_2O) or to that of the $NaPSS_d$ group (pure D_2O).

2.2 Small-angle neutron scattering

Small-angle neutron scattering (SANS) was performed both at the Orphée reactor in Saclay on the PACE spectrometer and at ILL in Grenoble on the D11 spectrometer. Wavelengths of $\lambda = 0.5$ and 1 nm and sample to detector distances of 1.9 and 4.7 m, respectively, were used on PACE spectrometer. Wavelength of $\lambda = 0.6$ nm and sample to detector distances of 1.1, 5.0 and 20.0 m were used on D11 spectrometer. The sample cells were, in all cases, quartz cells of inner thickness 2 mm. The scattered intensities were corrected for the parasitic intensity scattered by the quartz cell by subtraction and normalized to the water scattered intensity. The solvent scattering intensity was also subtracted. After these operations, the remaining signal is essentially due to the coherent scattering of the polymer in solution. The incoherent scattering due to the polymer was found to be negligible both by calculation and measurements [10].

3 Results and discussion

3.1 Association of copolymers

Association of copolymers was checked by neutron scattering on solutions in pure D_2O where the $NaPSS_d$ group is invisible. A typical scattering curve obtained in such a solvent is shown in Figure 1 for the 251/52 copolymer. At low scattering vectors q [22], the signal exhibits an interaction peak (q_1^*) that we attribute to correlations between positions of PEP groups. A second peak (q_2^*) is also observed. This second peak is an harmonic of the first interaction peak since $q_2^*/q_1^* = 1.7 \pm 0.1$ which is close to 1.8, the value observed in simple liquids [23], corresponding to next-nearest neighbour interactions. We must note that q_2^* is not observed for the 590/43 copolymer. The evolution of these peaks with the polymer concentration will be discussed in the last part of this paper. The scattered intensity at high scattering vectors is consistent with the scattering of spheres which indicates a

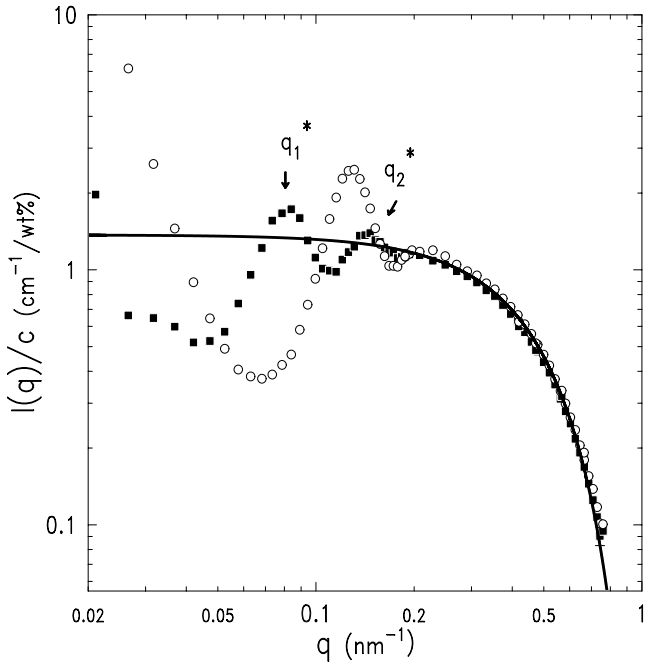

Fig. 1. Neutron-scattered intensity $I(q)/c$ *versus* q for the 251/52 copolymer without added salt, in a solvent that matches the NaPSS$_d$ group, at two different polymer concentrations: $c = 0.4$ wt% (squares), $c = 1.9$ wt% (circles). Typical interaction peaks between first and next-nearest neighbours are seen at q_1^* and q_2^* (indicated by arrows for $c = 0.4$ wt%), respectively. At high scattering vectors, the interaction between PEP groups becomes negligible and the scattered signal is concentration independent. This signal can be fitted by the form factor of a sphere (full line) of radius $R = 4.5 \pm 0.1$ nm, with an asymptotic intensity ($q \to 0$) in good agreement with an aggregation number of order 54. The observed excess scattering at $q \to 0$ can be related to the presence of few large aggregates.

self-association into spherical cores of PEP groups (Fig. 1). A similar behavior is observed for the 590/43 copolymer, again showing a self-association of PtBS groups into spherical cores. An average value of the core radius is found to be $R_c = 4.5 \pm 0.1$ nm for the 251/52 copolymer over a large concentration range (from 0.4 to 9.15 wt%) and found to be $R_c = 4.1 \pm 0.1$ nm for the 590/43 copolymer also over a large concentration range (from 1.9 to 15 wt%). These values are confirmed by Kratky plots ($q^2 I(q)$ *versus* q representation) and by Porod plots ($q^4 I(q)$ *versus* q representation) [24], of the same data for the same large concentration range. This indicates that the core shapes are concentration independent. In such a way, those solutions can be viewed as colloids, in water, stabilized by grafted polymer chains. The aggregation numbers can be evaluated using a model of homogeneous dense cores. Using the density expression for such a dense core, we obtain the aggregation number:

$$p = \frac{\mathcal{N}_A \rho_c V_c}{M_{wc}}, \tag{1}$$

where $\mathcal{N}_A$ is the Avogadro number, ρ_c the neutral moiety melt density (equal to 0.85 g/cm^3 and 0.95 g/cm^3 for the PEP and PtBS moieties, respectively), M_{wc} the neutral moiety molecular mass and $V_c = (4\pi/3)R_c^3$ the core volume.

Aggregation numbers of 54±1 and 23±3 for the 251/52 copolymer and the 590/43 copolymer are obtained, respectively. These values can be crosschecked since the absolute intensity (in cm^{-1}) scattered by cores at $q = 0$ is

$$I_{abs} = b^2 N^2 p \rho_s c \mathcal{N}_A / M_w, \tag{2}$$

where b is the neutral moiety contrast length in the solvent, N the degree of polymerization of the neutral moiety, p the aggregation number, ρ_s the solvent density, c the polymer concentration in g/g and M_w the molecular mass of a copolymer chain. The fit, at high scattering vectors, with the form factor of a sphere (Fig. 1) exhibits an asymptotic value ($q \to 0$) [22] in agreement with the absolute intensity deduced from equation (2).

Dynamic light scattering (DLS) on very dilute solutions (< 0.04 wt%) confirms the association and also provides the hydrodynamic radius of whole micelles, R_{hm}, according to a method described elsewhere [4], of about 38 ± 3 nm and 110 ± 10 nm for the 251/52 copolymer and the 590/43 copolymer, respectively. These hydrodynamic radii and the aggregation numbers lead to an overlap concentration c^* of the micelles:

$$c^* = \frac{p M_w}{\mathcal{N}_A V_m}, \tag{3}$$

where p is the aggregation number, M_w the molecular mass of a copolymer chain and $V_m = (4\pi/3)R_{hm}^3$ the micelle volume.

Such calculation gives c^* around 2 wt% and 0.1 wt% for the 251/52 copolymer and the 590/43 copolymer, respectively.

3.2 Structure of the charged corona

In a solvent which makes only the NaPSS$_d$ visible, the scattered intensity is essentially due to the scattering of PSS$_d$ monomers. Indeed, in neutron scattering, the contribution of counter-ions Na is negligible since their contrast is far lower than the PSS$_d$ monomer contrast. The scattering in such a mixture is shown in Figure 2 for the 251/52 copolymer in the dilute regime (the polymer concentration c is below c^*). At high scattering vectors (above $q \sim 0.5$ nm^{-1}), the signal is mainly due to fluctuations of the monomer profile, thus revealing the statistics of individual chains [25–27]. This signal, concentration independent, is found to be close to q^{-1}, which indicates a local statistics of nearly rod-like monomers. The limit of this q^{-1} behavior, $q_0 \sim 0.5$ nm^{-1}, can be related to the grafting distance ξ. Indeed, the area per charged chain ξ^2 can be calculated from

$$\xi^2 = 4\pi \frac{R_c^2}{p}, \tag{4}$$

where R_c is the measured core radius and p the aggregation number deduced from equation (1).

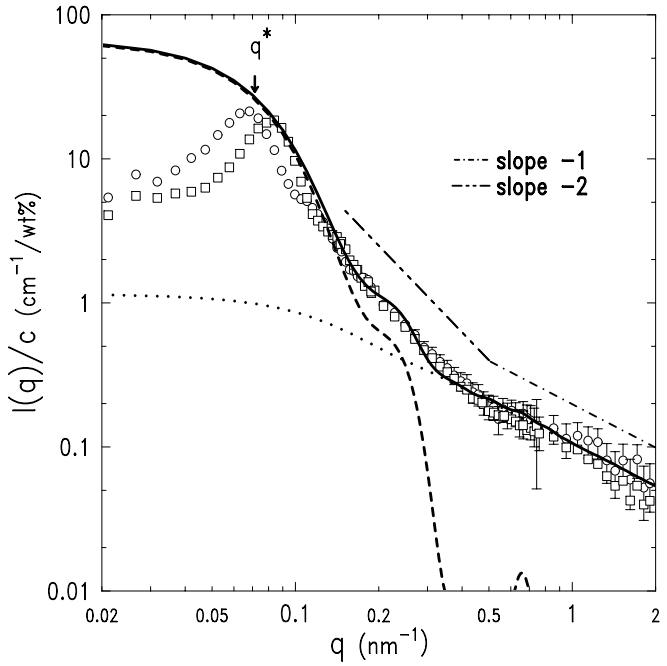

Fig. 2. Neutron-scattered intensity $I(q)/c$ *versus* q for the 251/52 copolymer without added salt, in a solvent which makes only the NaPSS$_d$ group visible, at two concentrations below the overlap concentration $c^* \sim 2\,\mathrm{wt\%}$: $c = c^*/10$ (circles) and $c = c^*/4$ (squares). The extended average conformation of charged corona chains is shown by the q^{-1} behavior (dot and dashed line) and by the q^{-2} behavior (dot-dot and dashed line). The q^{-1} behavior corresponds to a local statistics of rod-like monomers. The q^{-2} behavior corresponds to the superimposition of the centrosymmetric average density profile of rod-like chains and of the fluctuating profile due to the local statistics of rod-like chains. Above $q = 0.15$ nm^{-1}, experimental curves can be modeled by the intensity expressed in equation (6) (full line) with $R_c = 4.5$ nm, $L = 33.5$ nm and $p = 54$ for both concentrations. We have indicated the centrosymmetric average density profile contribution (dashed line) and the local statistics contribution (dotted line) of the fit. The interaction peak q^* is indicated by an arrow for $c = c^*/10$.

This leads to a grafting distance ξ around 2 nm, for the 251/52 copolymer, which is in agreement with $q_0\xi \sim 1$. This confirms that the q^{-1} behavior ($q\xi \geq 1$) corresponds to the statistics of individual nearly rod-like chains. At intermediate scattering vectors, from $q = 0.15\,\mathrm{nm}^{-1}$ to $q = 0.5\,\mathrm{nm}^{-1}$, the scattered signal can be written as the sum of two terms [5,25–27]. This sum originates from the decomposition of the monomer profile into two terms: a centrosymmetric average monomer profile and a fluctuating profile which reflects the heterogeneity of the corona [25,26].

The scattered signal can then be modeled by

$$I_F(q)/c = K\left[\alpha P_{\mathrm{ave}}(q) + \beta P_{\mathrm{ind}}(q)\right], \qquad (5)$$

where $P_{\mathrm{ave}}(q)$ is the scattering function of the average profile of monomers, $P_{\mathrm{ind}}(q)$ the form factor of an individual chain of the corona which approximates the scattering by the fluctuating profile [5,25–27], c the polymer concentration in g/g and $K = N_s^2\rho_s b^2\mathcal{N}_A/M_w$ with b the corona chain contrast length in the solvent, N_s the degree of polymerization of corona chains, ρ_s the solvent density, M_w the molecular mass of a copolymer chain. The values of the constants α and β are found by requiring that $I_F(q)/c$ extrapolates to Kp when $q \to 0$ (proportional to the mass of the micelle), thus giving $\alpha + \beta = p$ and requiring that the fluctuating part of the intensity extrapolates to K (proportional to the mass of a single chain), thus giving $\beta = 1$. This leads to

$$I_F(q)/c = K\left[(p-1)P_{\mathrm{ave}}(q) + P_{\mathrm{ind}}(q)\right]. \qquad (6)$$

An analoguous presentation of this decomposition can be found on p. 162 of reference [24].

The function $P_{\mathrm{ave}}(q)$ is given by the square of the normalized Fourier transform of the centrosymmetric density profile of the corona $\phi(r)$ [5]:

$$P_{\mathrm{ave}}(q) = \left[F(q,R,R_c)\right]^2 \qquad (7)$$

with

$$F(q,R,R_c) = \frac{\int_{R_c}^{R}[\phi(r)\sin(qr)r^2/qr]\mathrm{d}r}{\int_{R_c}^{R}\phi(r)r^2\mathrm{d}r},$$

where $L = R - R_c$ is the corona height.

Since experimental curves (Fig. 2) exhibit a q^{-1} behavior, we choose $\phi(r) \sim p/r^2$, the centrosymmetric density profile of a corona with rod-like arms [5]. Consistently, we take $P_{\mathrm{ind}}(q)$ to be the form factor of a rod-like chain of negligible thickness [24]:

$$P_{\mathrm{ind}}(q) = \left(\frac{2}{qL}Si(qL) - \left(\frac{\sin(qL/2)}{qL/2}\right)^2\right), \qquad (8)$$

where L is the rod length (here $L = R - R_c$).

Such a scattering from the corona, $I_F(q)/c$, is represented in Figure 2 with $R_c = 4.5$ nm (core radius of the 251/52 copolymer), $L = 33.5$ nm and $p = 54$ (aggregation number of the 251/52 copolymer). This scattering is consistent with the observed signal above $q = 0.15$ nm^{-1}. This confirms the extended statistics of charged chains. The whole micelle radius deduced $R = L + R_c = 38$ nm is in full aggreement with the whole micelle hydrodynamic radius R_{hm} previously observed for the 251/52 copolymer.

At low scattering vectors, an interaction peak is visible (q^*) and corresponds to the interaction between charged coronae. This is an indication of the micelle packing order, its evolution as a function of the polymer concentration will be discussed below. The existence of this peak at $c^*/10$, shows that such systems are strongly ordered by electrostatic interactions even for polymer concentrations below the overlap concentration.

3.3 Ordering between micelles

Interactions between micelles are modified when the polymer concentration is strongly increased ($c \gg c^*$).

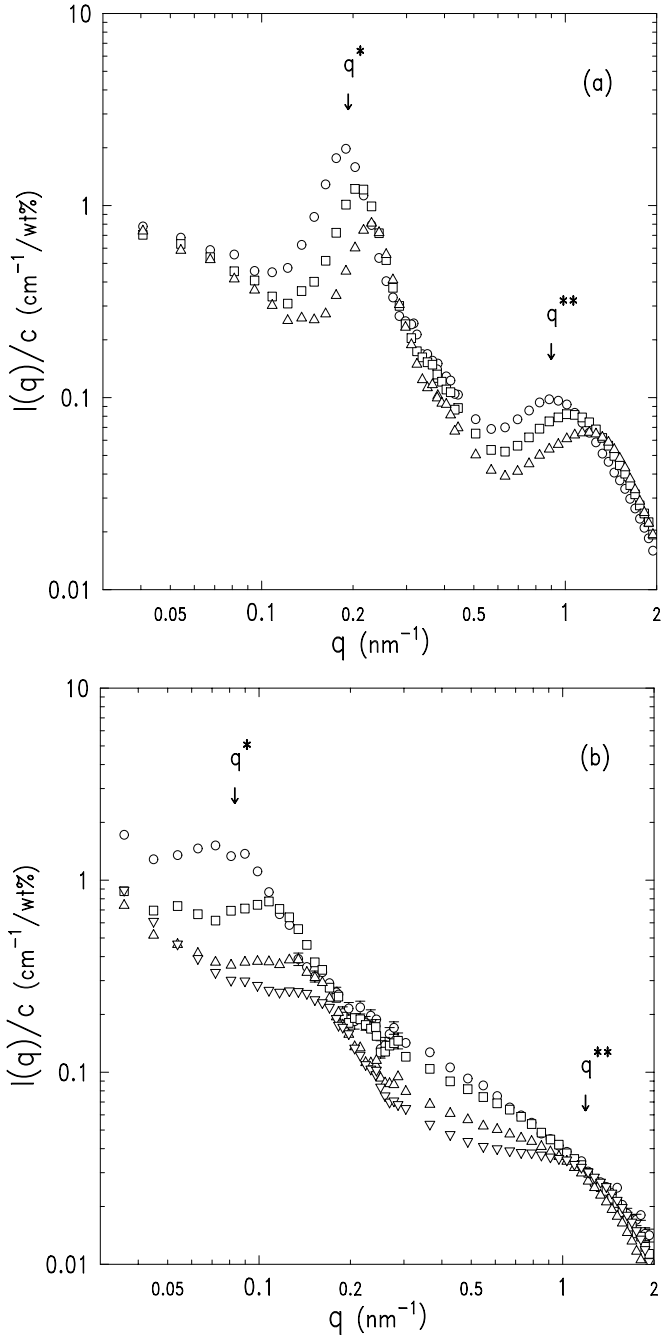

Fig. 3. Neutron-scattered intensity $I(q)/c$ *versus* q without added salt at concentrations above the overlap concentration c^*. (a) For the 251/52 copolymer ($c^* \sim 2\,\mathrm{wt\%}$), in a solvent which makes only the corona visible, at: $c = 5c^*$ (circles), $c = 7.5c^*$ (squares), $c = 10c^*$ (triangles). (b) For the 590/43 copolymer ($c^* \sim 0.1\,\mathrm{wt\%}$), in a solvent which makes only the corona visible, at concentrations strongly above c^*: $c = 20c^*$ (circles), $c = 50c^*$ (squares), $c = 100c^*$ (triangles), $c = 145c^*$ (inverted triangles). The coexistence of two interaction peaks, q^* and q^{**}, is shown for both copolymers. These peaks are indicated by arrows for $c = 5c^*$ in (a), for $c = 20c^*$ (q^*) and for $c = 145c^*$ (q^{**}) in (b). The interaction peaks are sharper for the 251/52 copolymer than for the 590/43 copolymer. The second interaction peak appears at higher concentration (relative to c^*) for the 590/43 copolymer than for the 251/52 copolymer.

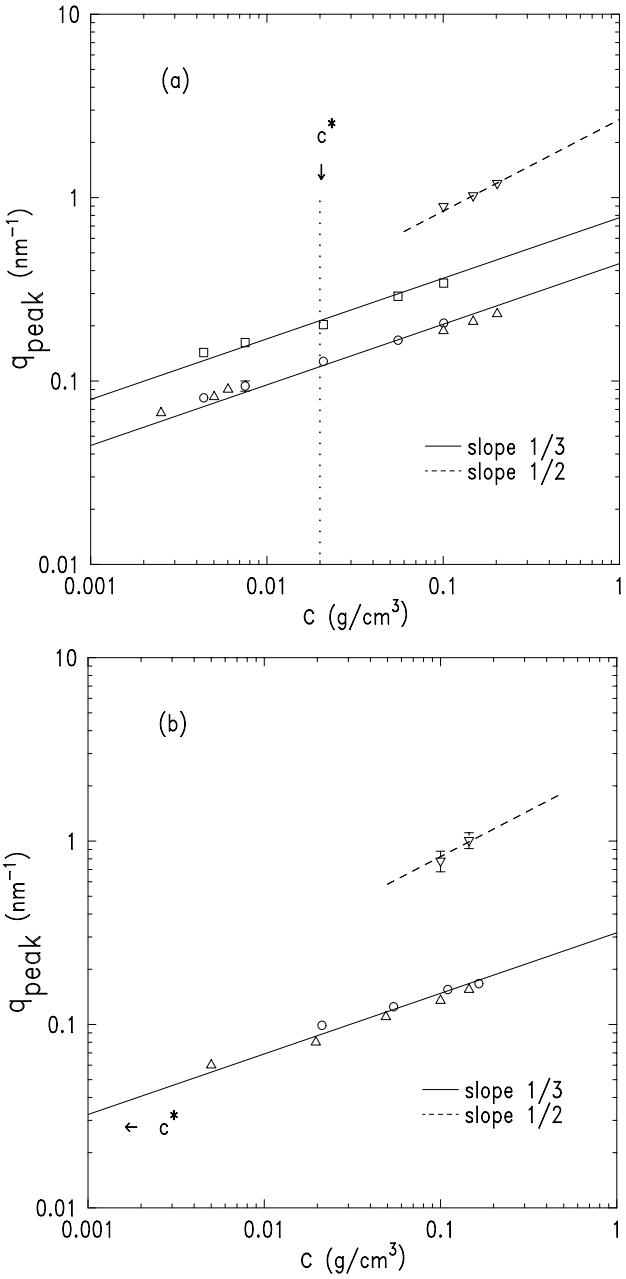

Fig. 4. Scattering vector q_{peak} *versus* polymer concentration c, in solvents that match the NaPSS_d group, the PEP group or the PtBs group. (a) For the 251/52 copolymer: q_1^* (circles) and q_2^* (squares) for the core ordering (see Fig. 1), q^* (triangles) and q^{**} (inverted triangles) for the corona ordering (see Fig. 2 and Fig. 3). (b) For the 590/43 copolymer: q_1^* (circles) for the core ordering, q^* (triangles) and q^{**} (inverted triangles) for the corona ordering (see Fig. 3). The first ordering peak (q^*, q_1^*) goes like $c^{1/3}$ over a wide concentration range spanning from the dilute regime to the concentrated regime. This is an indication of the micelle packing order . This is confirmed by the evolution of q_2^* also in $c^{1/3}$ since q_2^* corresponds to interactions with next-nearest neighbours. The second ordering peak observed in concentrated regime (q^{**}) is consistent with an evolution as $c^{1/2}$ despite of the narrow scattering vector range. Such an evolution is typical of polyelectrolyte semi-dilute solutions (homopolymers).

The behavior over such a concentration range, of the 251/52 copolymer and of the 590/43 copolymer is shown in Figure 3. The solvent contrast matches core neutral chains. The signal exhibits an interaction peak at q^*, corresponding to the ordering peak shown in the dilute regime. A second peak appears at higher scattering vectors q^{**} and coexists with the first ordering peak for both copolymers. This peak appears at much higher concentration (relative to c^*) for the 590/43 copolymer than for the 251/52 copolymer. It suggests two distinct behaviors when the polymer concentration is above c^*. A striking result for the 590/43 copolymer is that the peak q^* exists at concentrations strongly above c^*.

As we have shown, such spherical polyelectrolyte brushes exhibit interaction peaks in the dilute regime and in the concentrated regime. The origin of these interaction peaks can be tested by plotting their scattering vectors as a function of the polymer concentration. For both copolymers, we have reported in Figure 4, the scattering vectors of the interaction peaks from the core (see Fig. 1) and the scattering vectors of the interaction peaks from the corona (see Fig. 2 and Fig. 3) as a function of the polymer concentration. In this $q_{\rm peak}$ *versus* c representation, where $q_{\rm peak}$ is the scattering vector of the peaks and c the polymer concentration in g/cm^3, the ordering peaks q^* and q_1^* go like $c^{1/3}$. This is typical of liquid-like order. This is confirmed by the evolution of q_2^*, since it also goes like $c^{1/3}$, and since $q_2^*/q_1^* = 1.7 \pm 0.1$ which is consistent with liquid-like second order. The peak q_2^* is not observed for the 590/43 copolymer, because of the low aggregation number of this copolymer, $p \sim 23$, which can induce more disorder due to the sparser density of the brush. In this case, the liquid-like second order probably washes out. These peaks are related to the micelle packing order and are inversely proportional to the center-to-center distance between micelles. We note that the spherical geometry is confirmed since q_1^* and q^* are identical. A striking result is that such liquid-like order between charged brushes can be observed over a wide concentration range spanning from the dilute regime to the concentrated regime.

The ordering peak q^{**} for the 251/52 copolymer exists for $c \geq c^*$ at higher scattering vectors (Fig. 3). We attribute this peak to correlations similar to those encountered in polyelectrolyte homopolymer semi-dilute solutions [28]. In the latter case both experiments and theories [29] show that the peak evolves as $c^{1/2}$ at sufficiently high concentrations. Such an evolution is fully compatible with our data (Fig. 4) although the available scattering vector range is too narrow in order to deduce unambiguously any power law. Moreover, the absolute positions of the q^{**} peaks are in quantitative agreement with the positions of the peaks in the homopolyelectrolyte case at the very same concentrations [28]. A similar peak has been also reported for polyelectrolyte star solutions [30] and planar charged brushes [31]. Another origin of the peak could be found in the hydrophobic nature of the polymer backbone as suggested for weakly charged polyelectrolytes [32]. However, the peak positions are not at all in agreement with our data at comparable concentrations [33].

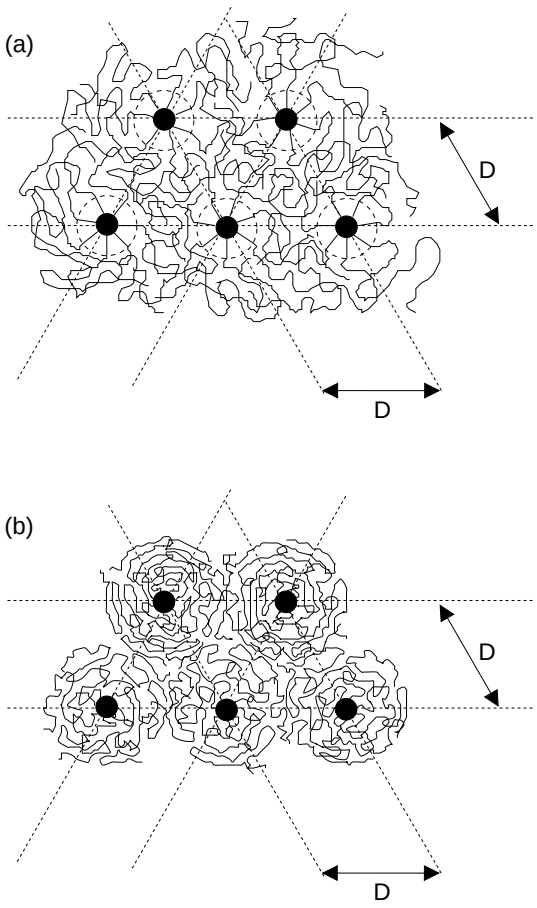

Fig. 5. Limiting cases of the corona interpenetration and of the chain contraction for a dense brush above c^*: (a) Interpenetration of coronae and formation at their periphery of a polyelectrolyte semi-dilute solution. The structure is ordered with a distance from center to center D and the nearly rod-like statistics of chains is conserved inside the non-interpenetrated volume (dashed circles). (b) Contraction of corona chains and formation of a polyelectrolyte semi-dilute solution inside each corona. The structure is ordered with a distance from center to center D and the polymer concentration is the new overlap concentration of the solution.

The appearance of the polyelectrolyte correlations at small scale in the concentrated regime may be of two distinct origins: an inter-coronae origin or an intra-corona origin. The first scenario implies the interpenetration of coronae and the formation of a polyelectrolyte semi-dilute solution at their periphery, giving rise to the correlations at high wave vectors. The second scenario is the contraction of corona arms, giving rise to a semi-dilute solution of less extended polyelectrolyte chains inside each corona. Following the latter scenario, it is understandable that the micelles stay liquid-like ordered as observed. Recent models predict such contraction inside polyelectrolyte star solutions [13]. The two limiting cases of full interpenetration and full contraction are depicted in Figure 5a and b.

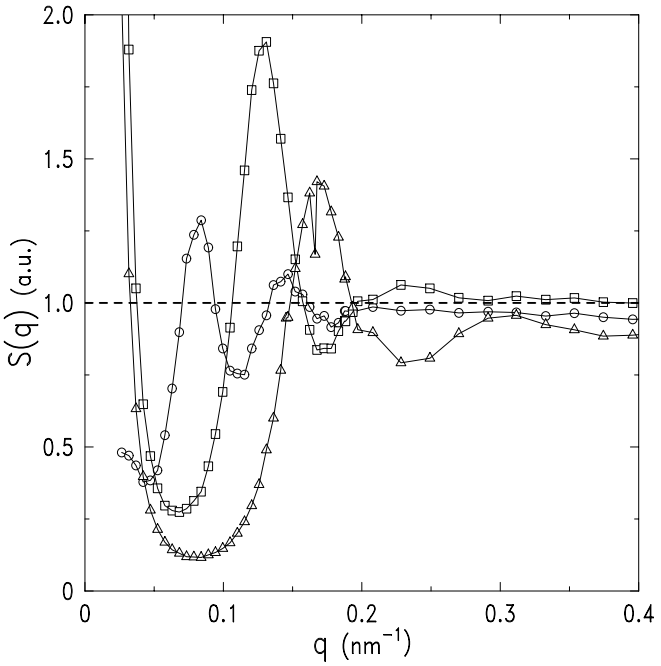

Fig. 6. Structure factor $S(q)$ *versus* q for the 251/52 copolymer, deduced following the method depicted in the text, at three different concentrations below, at and above $c^* \sim 2\,\mathrm{wt}\%$: $c = c^*/5$ (circles), $c = c^*$ (squares), $c = 2.5c^*$ (triangles). The maximum intensity of $S(q)$ undergoes a maximun at $c = c^*$.

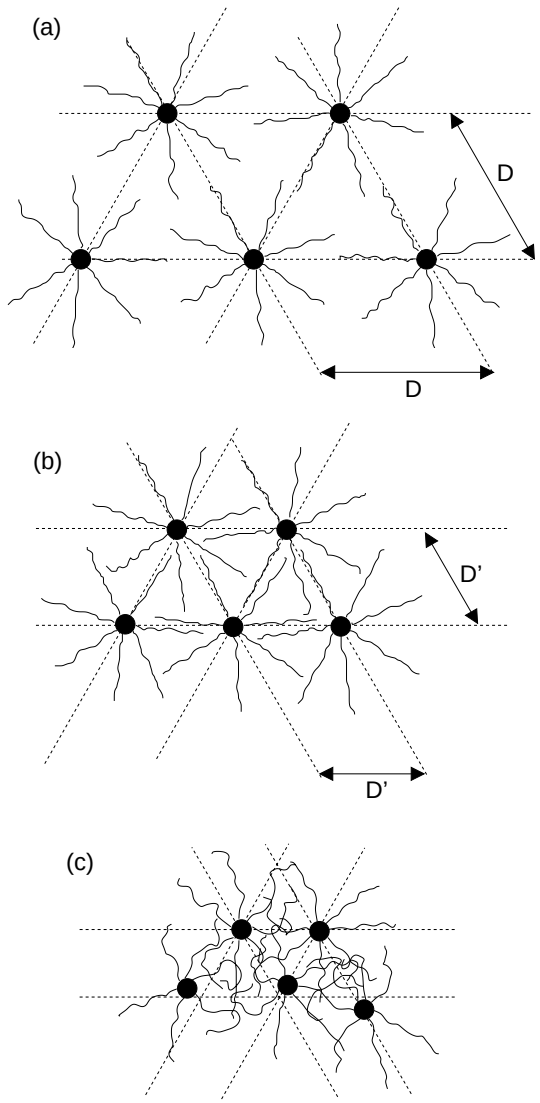

Fig. 7. Schematic possible model of the sparsely dense brush behavior above c^*: (a) $c = c^*$, the corona chain conformation is rod-like and the structure is ordered with a distance from center to center $D = 2R$. (b) $c^* < c < c^{**}$, the coronae interpenetrate each other but the chain conformation stays rod-like. The structure stays ordered with a distance from center to center $D' < D$. (c) $c > c^{**}$, the interpenetrated volume becomes too dense. The corona chains interpenetrate each other and the order could begin disappearing.

Since the core size is constant, the scattered signal $I(q)$ at all concentrations (in solvents which make only the cores visible (Fig. 1)) can be divided by the form factor $P(q)$ associated to the spherical core to provide the overall structure factor $S(q)$ (since $I(q)/c \propto S(q)P(q)$). Such structure factors are presented in Figure 6 for the 251/52 copolymer. This $S(q)$ *versus* q representation shows that the maximum intensity of the structure factor undergoes a maximum at $c = c^*$. This situation is reminiscent of the situation encountered with neutral polymer stars and could constitute an argument in favor of the corona interpenetration, which is favored from the current studies on neutral polymer stars [34]. Indeed at the onset of interpenetration, a maximum in osmotic pressure is predicted [35]. However in the charged case, interactions between micelles have also an electrostatic contribution in addition to the osmotic contribution. The presence of charges can lead to a more complex behavior also exhibiting a maximum intensity of the structure factor at c^*.

Our results do not allow us to distinguish whether the polyelectrolyte correlations are due to an interpenetration of coronae or due to a contraction of chains inside these coronae. This puzzling question remains open.

For the 590/43 copolymer, the absolute values of the q^{**} peaks are identical to those found with the 251/52 copolymer, at the same concentration. This strengthens the interpretation in terms of polyelectrolyte correlations. Again, the very limited number of data points does not allow us to check the validity of the $c^{1/2}$ variation although our data are compatible with it. Moreover, Figure 3 suggests that the corona conformations of the 590/43 copolymer and of the 251/52 copolymer are not the same when the concentration is above c^*. Indeed, this figure shows that the polyelectrolyte correlations appear at much higher concentration (relative to c^*) for the 590/43 copolymer than for the 251/52 copolymer. We know also that the local conformation of corona chains is fully extended, for the 590/43 copolymer, at a concentration as high as $c = 10c^*$ [10]. Moreover, the overall packing order of the 590/43 copolymer seems to progressively disappear while the polyelectrolyte correlations increase in contrast with the 251/52 copolymer which stays strongly ordered.

Indeed as observed in Figure 3, the q^* peaks of the 590/43 copolymer begin larger while the polyelectrolyte correlations increase in contrast with the q^* peaks of the 251/52 which stay identical. These differences can be explained by the difference in the brush density, *i.e.* by the differences in the aggregation number and in the degree of polymerization of the charged moiety.

The 251/52 copolymer has a dense corona with an aggregation number of 54 ± 1. This suggests that above c^*, the rod-like statistic of the chains begins to disappear by interpenetration or by contraction as explained above (Fig. 5). The 590/43 copolymer has a relatively low aggregation number, 23 ± 3 more than twice less that of the 251/52 copolymer, with a degree of polymerization 2.5 times longer. A possible explanation is that such sparsely dense brushes interpenetrate each other without changing their chain statistics (rod-like statistics), as if a more dense brush could be created at the corona periphery, over a large concentration range from c^* to a concentration c^{**} (Fig. 7). We can estimate c^{**} between $c = 30c^*$ and $c = 50c^*$ (Fig. 3 and [10]). Above c^{**}, the interpenetrated volume would become too dense, the formation of a polyelectrolyte semi-dilute solution appears progressively by interpenetration of chains (Fig. 7) and the liquid-like order could begin disappearing.

4 Summary and conclusion

In this paper, we have studied the scattering intensity of spherical charged brushes formed by charged-neutral diblock copolymers both in the dilute and concentrated regimes. The conformation of such brushes is found to be fully extended in the dilute regime. We have shown that, at intermediate scattering vectors the scattering intensity exhibited a quasi-q^{-2} behavior corresponding to the superimposition of the centrosymmetric average density profile of rod-like chains and of the fluctuating profile due to the local statistics of rod-like chains. At high scattering vectors a quasi-q^{-1} behavior is observed, corresponding to fluctuations of the monomer profile due to the local statistic of rod-like monomers. Such solutions exhibit strong liquid-like order over a wide concentration range spanning from the dilute regime to the concentrated regime. At high concentration, polyelectrolyte correlations appear and coexist with the liquid order. However our results show a strong dependence of the brush density on the evolution of the chain conformation and on the structure of solutions at concentrations above c^*. In particular, chains in less dense brushes exhibit extended statistics largely above c^*. The striking result for dense brushes is that the solutions stay very strongly ordered even when the polyelectrolyte order appears.

A natural extension of this work is to study the localization and the correlations of counter-ions, for such objects, as a function of the concentration [20] and of the brush density. Moreover, the study of overall structure factors should provide an interesting opportunity to deduce the interaction potential between micelles and separate the electrostatic and the osmotic contributions. This could bring about a better understanding of such solutions in the concentrated regime. Such work is currently in progress.

One of us (F.M.) thanks the région Charentes-Poitou for partial support. J.W.M. and M.T. acknowledge support of the National Science Foundation, CTS and DMR programs, Grant NSF-CTS-9616797. The manuscript benefited from a critical reading of M. Alba.

References

1. D. Kiserow, K. Prochazka, C. Ramireddy, Z. Tuzar, P. Munk, S.E. Webber, Macromolecules **25**, 461 (1992).
2. K. Khougaz, I. Astafieva, A. Eisenberg, Macromolecules **28**, 7135 (1995).
3. C. Amiel, M. Sikka, J.W. Schneider, Y.H. Tsao, M. Tirrell, J.W. Mays, Macromolecules **28**, 3125 (1995).
4. P. Guenoun, M. Delsanti, D. Gazeau, L. Auvray, D.C. Cook, J.W. Mays, M. Tirrell, Eur. Phys. J. B **1**, 77 (1998).
5. S. Förster, N. Hermsdorf, W. Leube, H. Schnablegger, M. Regenbrecht, S. Akari, P. Lindner, C. Böttcher, J. Phys. Chem. **103**, 6657 (1999).
6. P.G. de Gennes, P. Pincus, R.M. Velasco, F. Brochard, J. Phys. (Paris) **37**, 1461 (1976).
7. P. Guenoun, H.T. Davis, J.W. Mays, M. Tirrell, Macromolecules **29**, 396 (1996).
8. P. Pincus, Macromolecules **24**, 2912 (1991).
9. E.B. Zhulina, O.V. Borisov, Macromolecules **29**, 2618 (1996).
10. P. Guenoun, F. Muller, M. Delsanti, L. Auvray, Y.J. Chen, J.W. Mays, M. Tirrell, Phys. Rev. Lett. **81**, 3872 (1998).
11. J.L. Barrat, J.F. Joanny, Adv. Chem. Phys. **XCIV**, 1 (1996).
12. U. Micka, C. Holm, K. Kremer, Langmuir **15**, 4033 (1999).
13. O.V. Borisov, J. Phys. II **6**, 1 (1996).
14. G.S. Manning, J. Chem. Phys. **51**, 934 (1969).
15. F. Oosawa, *Polyelectrolytes* (M. Dekker, New York, 1971).
16. J. Ray, G.S. Manning, Langmuir **10**, 2450 (1994).
17. B.Y. Ha, A.J. Liu, Phys. Rev. Lett. **79**, 1289 (1997).
18. H. Schiessel, P. Pincus, Macromolecules **31**, 7953 (1998).
19. R.M. Nyquist, B.Y. Ha, A.J. Liu, Macromolecules **32**, 3481 (1999).
20. F. Muller, P. Fontaine, M. Delsanti, P. Lesieur, P. Guenoun, in preparation.
21. P.L. Valint, J. Bock, Macromolecules **21**, 175 (1988).
22. We observe at very small angle an excess intensity. Such an intensity can be related to the presence of very few larger aggregates which coexist with the single micelles. This question has been studied in similar systems in reference [4]. In the present paper, we do not consider this ubiquitous intensity at small angle for all extrapolations at $q \to 0$.
23. J.L. Yarnell, M.J. Katz, R.G. Wenzel, S.H. Koenig, Phys. Rev. A **7**, 2130 (1973).
24. J.S. Higgins, H.C. Benoit, *Polymers and Neutron Scattering* (Clarendon Press, Oxford 1994).
25. L. Auvray, C. R. Acad Sci. Paris **302 II**, 859 (1986).
26. L. Auvray, P.G. de Gennes, Europhys. Lett. **2**, 647 (1986).
27. C.M. Marques, D. Izzo, T. Charitat, E. Mendes, Eur. Phys. J. B **3**, 353 (1998).

28. W. Essafi, F. Lafuma, C.E. Williams, Eur. Phys J. B. **9**, 261 (1999).
29. See, for instance, M. Muthukumar, J. Chem. Phys. **105**, 5184 (1996); A. Yethiraj, C.Y. Shew, Phys. Rev. Lett. **77**, 3937 (1996); M. Dymitrowska, L. Belloni, J. Chem. Phys. **109**, 4659 (1998).
30. M. Rawiso, J. Phys. IV **9**, Pr1-147 (1999).
31. Y. Mir, PhD Thesis, Université Paris VII (1995).
32. J.F. Joanny, L. Leibler, J. Phys. **51**, 545 (1990).
33. A. Moussaid, F. Schosseler, J.P. Munch, S.J. Candau, J. Phys. II **3**, 573 (1993).
34. G.S. Grest, L.J. Fetters, J.S. Huang, D. Richter, Adv. Chem. Phys. **XCIV**, 67 (1996).
35. T.A. Witten, P. Pincus, M.E. Cates, Europhys. Lett. **2**, 137 (1986).